

The impact of road traffic on global tropospheric ozone

Claire Granier

Service d'Aéronomie, CNRS, Paris, France

Max Planck Institute for Meteorology, Hamburg, Germany

CIRES/Aeronomy Laboratory, NOAA, Boulder, Colorado, USA

Guy P. Brasseur

Max Planck Institute for Meteorology, Hamburg, Germany

National Center for Atmospheric Research, Boulder, Colorado, USA

Received 25 July 2002; revised 18 November 2002; accepted 12 December 2002; published 29 January 2003.

[1] Model calculations suggest that the emissions by road traffic (passenger vehicles and trucks) of ozone precursors (NO_x , CO, hydrocarbons) have a substantial impact on the concentration of tropospheric ozone at the regional scale in the boundary layer and at the hemispheric scale in the free troposphere. Increases in the surface ozone concentration resulting from road traffic are typically 5–15 % at mid-latitudes in the Northern hemisphere during summer. Similar levels of ozone changes are calculated in the Southern hemisphere during austral summertime, but with perturbations less uniformly distributed than in the Northern hemisphere. Ozone changes produced in the upper troposphere as a result of road traffic are of the same magnitude (5–8% in July) as the changes generated by commercial aircraft operations. A traffic-induced reduction of 3% is estimated for the globally and annually averaged lifetime of methane. **INDEX TERMS:** 0322 Atmospheric Composition and Structure: Constituent sources and sinks; 0368 Atmospheric Composition and Structure: Troposphere—constituent transport and chemistry. **Citation:** Granier, C., and G. P. Brasseur, The impact of road traffic on global tropospheric ozone, *Geophys. Res. Lett.*, 30(2), 1086, doi:10.1029/2002GL015972, 2003.

1. Introduction

[2] Over the past years, much attention has been given to the impact of chemical emissions provided by the fleets of aircraft in the upper troposphere/lower stratosphere [Brasseur *et al.*, 1996, 1998; IPCC, 1999] and of ships in the surface layer [Lawrence and Crutzen, 1999]. High temperature combustion of fossil fuels occurring in aircraft and ship engines leads to the release in the atmosphere of substantial amounts of nitrogen oxides, carbon monoxide and volatile organic compounds. In the presence of sunlight, photochemical catalytic cycles involving the presence of these compounds can produce ozone. Models have determined [IPCC, 1999] that, in response to commercial aircraft emissions, the global ozone burden below 15 km altitude should have increased by 3–10 Tg, or 1–3%, and upper tropospheric ozone in the Northern hemisphere should have increased by 2–14% in June–July during the period of highest photochemical activity, downstream and poleward of the principal traffic areas. At the surface in the North

Atlantic during July, the ozone concentration should perhaps have doubled in response to emissions by ship engines [Lawrence and Crutzen, 1999]. The chemistry of the hydroxyl radical (OH), and hence the “oxidizing power” of the atmosphere, as well as climate forcing should also have been affected.

[3] Since the studies of Haagen-Smit [1952] in Los Angeles, it is well known that the high ozone levels recorded in urban areas, mostly during summertime, result from the release of ozone precursors by automobiles, power plants and other industrial facilities. In spite of the measures taken to reduce traffic and industrial emissions, ozone pollution events are still often observed in North America, Europe and Asia. The purpose of the present paper is to highlight the importance of automobile emissions on global ozone. The present study focuses therefore only on large-scale impacts (i.e., hemispheric scale) and not on local or urban effects.

2. The Model

[4] To quantify large-scale effects of road traffic, we use the IMAGES global chemical transport model, which was described and evaluated by Müller and Brasseur [1995], and by Granier *et al.* [2000a, 2000b]. The resolution of the model is 5 degrees in latitude and longitude, so that only the effects with spatial scales of typically 500 km or more can be estimated. The model includes 25 altitude levels between the surface and 50 hPa, of which 8 are located in the boundary layer. Transport of long-lived chemical species is simulated by the Semi-Lagrangian advection scheme of Smolarkiewicz and Rasch [1991], driven by meteorological parameters provided by ECMWF analyses (averaged over the 1985–1989 period). Unresolved large scale eddies are parameterized by diffusion coefficients calculated from the climatological wind variances. Convective transport is parameterized by an array of probability transfer coefficients [Costen *et al.*, 1988] dependent on time and location of the convection as deduced from the International Satellite Cloud Climatology Project (ISCCP) data. Vertical transport associated to turbulence in the boundary layer is represented by vertical eddy diffusion. The chemical scheme, implemented in the model and mostly appropriate for remote and moderately polluted regions, is described by Müller and Brasseur [1995]. The primary hydrocarbons included in the scheme are ethane, propane, ethylene, propylene, isoprene, terpenes, and a lumped species that represents the contri-

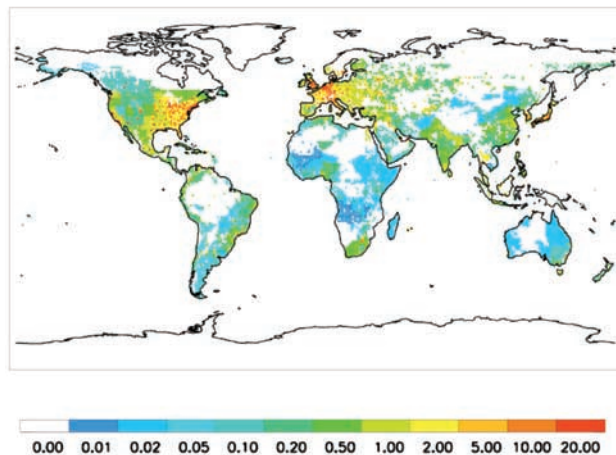


Figure 1. NO_x emissions (annual mean) from road traffic (year 1995) in 10^{10} molec cm^{-2} s^{-1} based on the EDGAR v2.0 inventory [Olivier *et al.*, 1996].

bution of all the other hydrocarbons. The model results have been extensively evaluated and compared with observations by Müller and Brasseur [1995], and Friedl [1997]. Müller and Brasseur [1995] have specifically examined the performance of IMAGES regarding vertical transport of tracers like radon-222 and have showed that the simulated concentrations of this species fall within the error bars of the measurements. Lamarque *et al.* [1996] have assessed the relative contributions of the different nitrogen sources to the tropospheric NO_x budget: the model simulations have suggested that the NO_x concentration in the southern hemisphere is mostly dominated by the lightning source, while the northern hemisphere odd nitrogen burden results mainly from the influence of fossil fuel combustion, aircraft and lightning emissions.

3. Emissions

[5] The model accounts for natural as well as human-induced emissions of key atmospheric compounds (including those related to fossil fuel consumption, industrial activities, biomass burning, vegetation and soil processes). Biomass burning emissions are similar to those described by Granier *et al.* [2000a], based on Hao and Liu [1994]. Biogenic emissions of isoprene and terpenes are taken from Guenther *et al.* [1995], and oceanic and soil emissions are from Müller [1992]. Anthropogenic emissions including emissions associated with road traffic (1×1 degree distribution) are specified according to the EDGAR version 2.0 inventory [Olivier *et al.*, 1996]. In the case of carbon monoxide, the emissions from automobiles and trucks (207 Tg CO per year) represent 67% of the anthropogenic (fossil fuel and industrial) emissions and 14% of the total emissions. In the case of NO_x (NO + NO₂), road traffic (emission of 9.6 Tg N per year) represents 40% of the fuel-related emissions and 24% of the total surface source (yearly average of 23 Tg N/year for energy-related sources, 10 Tg N/year for biomass burning including fuelwood use, 7 Tg N/year for soils). Atmospheric NO_x sources from lightning and commercial aircraft are assumed to account

for 5 and 0.5 Tg N/year, respectively. As shown by Figure 1 (in the case of NO_x), the emissions associated with road traffic are largest in western Europe, North America and Japan. Significant emissions, however, are also occurring in the region of the Persian Gulf, in India, eastern China, South Africa, Mexico, Brazil and southeastern Australia.

4. Results and Discussion

[6] Two model simulations have been performed, one in which road traffic emissions are included, and one in which these emissions are omitted. The model has been integrated for two years, and the results corresponding to the second year have been compared. Figures 2a–2d show the differences in the distribution of nitrogen oxides and ozone between these two simulations. In the case of nitrogen oxides (NO_x), the perturbations in the surface concentrations are predicted to be significant primarily in the vicinity of (and directly downwind from) the region with high traffic emissions, while the perturbations at higher altitudes, although smaller, are more uniformly distributed in space. This different behavior results directly from the fact that the chemical lifetime of NO_x increases with height (about 1 day

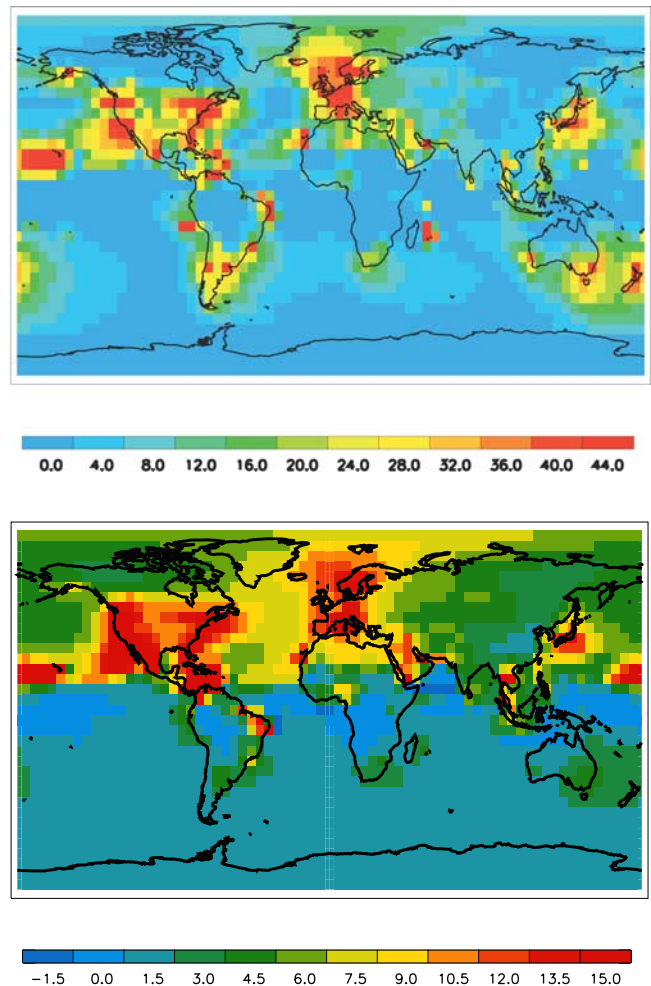


Figure 2. Percentage difference in the concentrations of NO_x (a) and ozone (b) at the surface and NO_x (c) and ozone (d) at 300 hPa due to road traffic (July conditions).

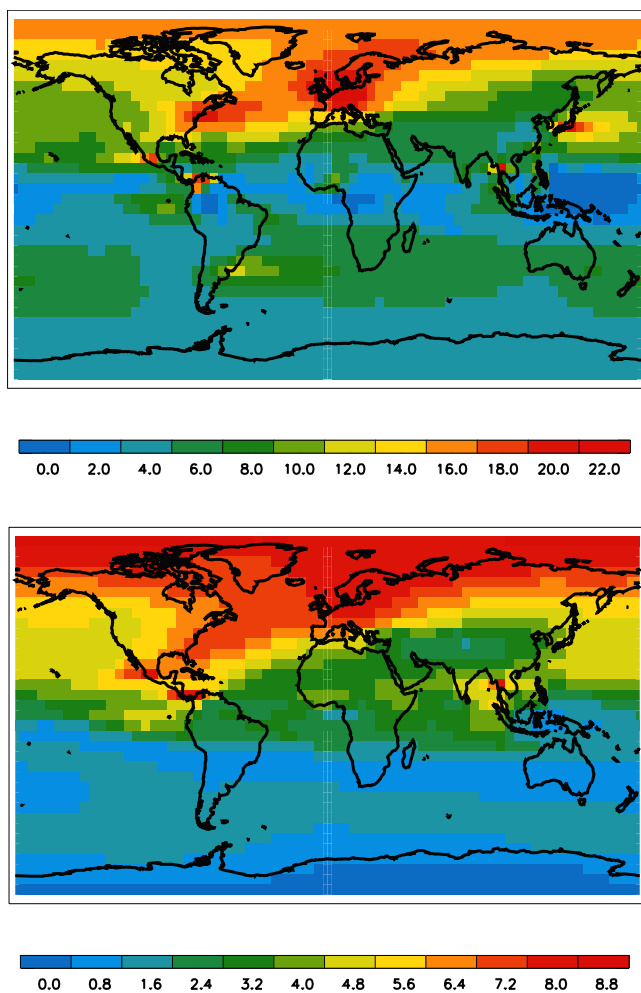


Figure 2. (continued)

at the surface and several weeks at 300 hPa). In July, the changes in the mean surface NO_x concentration (Figure 2a) are typically 0 to 4% (about 1 pptv) over the oceans, except in the vicinity of coastal regions and islands (e.g., Hawaii, Caribbean) where increases of about 35% (50 pptv) are predicted. Changes reach 30–40% (or 500 pptv) in the vicinity of the continental European and North American source areas. Ventilation to the free troposphere takes place in regions of high emissions and active convection. In the free troposphere at 500 hPa, the calculated NO_x changes reach maxima of 25% (30–50 pptv) in Western Europe and in the Eastern US. At 300 hPa, the NO_x enhancement (typically 10–20% or 15–30 pptv) is rather uniformly distributed in the mid- and high latitudes of the Northern hemisphere (Figure 2c). These estimates depend, however, on the model formulation adopted for boundary layer ventilation, convective transport and NO_x production by lightning. The factors that represent vertical atmospheric exchanges also affect the efficiency at which ozone is produced from the NO_x emissions, and hence the relative influence of the different NO_x sources for the global ozone budget. During wintertime in the Northern hemisphere (not shown), the changes in the NO_x concentrations at the surface reach higher maximum values (50–70% or 4–5

ppbv) and the perturbation is somewhat more spatially uniform than in summer since the chemical lifetime of NO_x is longer than during summertime.

[7] In July, typical increases in the mean surface concentration of carbon monoxide (CO) at the regional scale are 20–30% (30–50 ppbv) in the northeastern US and in Western Europe; it is about 8–10% (5 ppbv) in the region of the North Atlantic. At 500 and 300 hPa, the CO enhancement in the Northern hemisphere is rather uniformly distributed, and is typically 5–15% (6–12 ppbv). In January the perturbations in the surface concentration of the Northern hemisphere are largest and more uniformly distributed since the level of OH (which provides the major destruction of CO) is lowest during the winter season. The large-scale changes in CO concentrations produced by road traffic at the surface are typically 25% (or 20–25 ppbv) in January with regional maximum values reaching 35% or 80 ppbv in Europe and North America.

[8] The photochemical production of ozone is expected to be substantial during summer when the largest amount of solar radiation is available. For example at the surface in the Northern hemisphere during July, the change in the mean ozone concentration due to road traffic emissions is typically 10–15% (5–10 ppbv) in North America, Europe and Eastern Asia (Figure 2b). In remote areas such as Hawaii and the Caribbean where the background NO_x is low, the ozone production efficiency by NO_x is higher than in polluted regions like Europe and North America. As a result, the comparatively small emissions by road traffic lead to substantial relative ozone and OH increases. In the boundary layer, emissions by road traffic affect ozone at the regional scale. At 500 hPa and 300 hPa (Figure 2d), where the perturbations are more uniformly distributed in space (affecting the atmosphere at the hemispheric scale), the ozone increase in the Northern hemisphere (mid- and high latitudes) is typically 5–10% (3–5 ppbv) and 4–8% (4–6 ppbv), respectively. The ozone increase in the upper troposphere (Northern hemisphere, summertime) resulting from road traffic (9.6 Tg N/year) is therefore of similar magnitude as the ozone change produced by current commercial aircraft operations (0.6 Tg N/year). This is explained by the fact that the changes in the NO_x concentration near 300 hPa are similar for the aircraft emissions (primarily near the tropopause) and for the surface road traffic sources at the surface. Globally, the non-linearity in the ozone chemistry leads to different ozone production efficiencies for sources located at the surface and in the upper troposphere. Again, the uncertainties associated with the formulation of vertical exchanges should be emphasized.

[9] The spatial distribution of the ozone changes tends to be similar to that of the NO_x changes (since the photochemical ozone production is primarily NO_x-limited), although it is somewhat more uniform (since ozone has a longer chemical lifetime than NO_x). Note the increase in the surface ozone concentration (8% or 3 ppbv) in the North Atlantic resulting from road traffic-generated ozone precursors in the Eastern United States. In January, increases in surface ozone concentrations are always less than 4% north of 40°N with slight decreases (2%) occurring in the Eastern US and the industrialized areas of Western Europe, where ozone is titrated by nitrogen oxides. At all seasons, the changes are low (less than 2%) in the equatorial atmosphere,

especially near the Intertropical Convergence Zone (ITCZ), where the contribution of road traffic to ozone precursors is small.

[10] Finally during July, the change in the surface density of OH (not shown) is relatively large (typically 15–25% or $4\text{--}6 \cdot 10^5 \text{ cm}^{-3}$) in regions where NO_x concentrations have increased in response to road traffic, and specifically in the US, Europe, eastern Asia, Australia and the coastal areas of South America. At 500 hPa, the largest changes in the OH densities are found over the eastern US, the North Atlantic and western and northern Europe (typically 5–8% or $1.5\text{--}2.5 \cdot 10^5 \text{ cm}^{-3}$), and, in a more localized way, over Central America and south-east Asia (typically 5–10% or $1\text{--}2 \cdot 10^5 \text{ cm}^{-3}$). At 300 hPa, the OH change generated by road transport is never larger than 2% or $2 \cdot 10^5 \text{ cm}^{-3}$. In January, surface OH decreases substantially in response to automobiles and trucks emissions in the highly polluted regions of Europe and North America where the background nitrogen oxide level is so high that additional NO_x tends to convert substantial quantities of HO_x into nitric acid [see e.g., Logan *et al.*, 1981]. A similar situation is observed in Western Europe during summer. The change in the mean “oxidizing capacity” of the atmosphere can be characterized by the change in the globally and annually averaged photochemical lifetime of long-lived source gases. Our model shows that, in response to road traffic, the global lifetime (ratio of the total tropospheric burden to the total tropospheric loss) of methane and methylchloroform has decreased by approximately 3%.

5. Summary and Conclusions

[11] Calculations performed with a global chemical transport model (IMAGES) suggest that road traffic enhances surface ozone concentrations not only in the vicinity of emission sources, but also in remote areas of the northern hemisphere in July and in large areas of both hemispheres in January. Significant changes are predicted not only in the planetary boundary layer but also in the free troposphere. Emissions by road traffic lead therefore to ozone pollution not only in the vicinity of precursors sources, but also at the hemispheric scale. During summertime, the total impact of road traffic on surface ozone is estimated to be almost 15% in Europe and North America (eastern and western US). It reaches about 8% in the North Atlantic, 5% in the North Pacific, 4% in Siberia and China, and 12% in Japan. Note, however, that these perturbations are expressed as relative values, due to the spatial heterogeneity in the global ozone distribution. Ozone perturbations in the mid- and upper troposphere are typically 5–10%, i.e., comparable to the changes expected from the current fleet of commercial aircraft [Brasseur *et al.*, 1996, 1998]. Further studies will address the combined effects of all types of transportation. A limitation associated with current global chemical-transport models is their inability to resolve highly concentrated plumes of pollutants with consequences on the calculation of the mean ozone production in a single model grid element. Higher resolution models with regional capability are therefore required to more accurately quantify the

impact of traffic on the tropospheric composition, especially in the vicinity of polluted areas.

[12] **Acknowledgments.** We thank Matthias Beekmann and Baerbel Langemann for comments on the manuscript and Jean-François Müller for providing the latest version of the IMAGES model. Constructive remarks by the anonymous reviewers are also acknowledged. This work was partly funded by the European Commission under contract EVK2-1999-0011 and by the German BMBF under project ISOTROP. The National Center for Atmospheric Research is sponsored by the National Science Foundation.

References

- Brasseur, G. P., J.-F. Müller, and C. Granier, Atmospheric Impact of NO_x Emissions by Subsonic Aircraft: A Three-dimensional Study, *J. Geophys. Res.*, **101**, 1423–1428, 1996.
- Brasseur, G. P., R. A. Cox, D. Hauglustaine, I. Isaksen, J. Lelieveld, D. H. Lister, R. Sausen, U. Schumann, A. Wahner, and P. Wiesen, European scientific assessment of the atmospheric effects of aircraft emissions, *Atmos. Environ.*, **32**, 2327–2422, 1998.
- Costen, R. C., G. M. Tennille, and S. J. Levine, Cloud pumping in a one-dimensional model, *J. Geophys. Res.*, **93**, 15,941–15,954, 1988.
- Friedl, R., (ed), Atmospheric effects of subsonic aircraft: Interim assessment report of the Advanced Subsonic Technology Program, *NASA Reference Publication 1400*, 143 pp., Washington, D.C., 1997.
- Granier, C., G. Pétron, J. F. Müller, and G. Brasseur, The impact of natural and anthropogenic hydrocarbons on the tropospheric budget of carbon monoxide, *Atmos. Env.*, **34**, 5255–5270, 2000a.
- Granier, C., J. F. Müller, G. and Brasseur, The impact of biomass burning on the global budget of ozone and ozone precursors, in *Biomass burning and its inter-relationships with the climate system*, edited by J. L. Innes, M. Beniston, and M. M. Verstraete, pp. 69–85, Kluwer Academic Publishers, 2000b.
- Guenther, A., C. N. Hewitt, D. Erickson, R. Fall, C. Geron, T. Graedel, P. Harley, L. Klinger, M. Lerdau, W. McKay, T. Pierce, B. Scholes, R. Steinbrecher, R. Tallamraju, J. Taylor, and P. Zimmerman, A global model of natural volatile organic compound emissions, *J. Geophys. Res.*, **100**, 8873–8892, 1995.
- Haagen-Smit, A. J., Chemistry and physiology of Los Angeles Smog, *Ind. Eng. Chem.*, **44**, 1342–1346, 1952.
- Hao, W. M., and M. H. Liu, Spatial and temporal distribution of tropical biomass burning, *Global Biogeochem. Cycles*, **8**, 495–503, 1994.
- Intergovernmental Panel on Climate Change (IPCC), Aviation and the Global Atmosphere, edited by J. E. Penner, D. H. Lister, D. J. Griggs, D. J. Dokken, M. McFarland, Cambridge University Press, UK, 373 pp., 1999.
- Lamarque, J.-F., G. P. Brasseur, P. G. Hess, and J.-F. Müller, Three-dimensional study of the relative contributions of the different nitrogen sources in the troposphere, *J. Geophys. Res.*, **101**, 22,955–22,968, 1996.
- Lawrence, M. G., and P. J. Crutzen, Influence of NO_x emissions from ships on tropospheric photochemistry and climate, *Nature*, **402**, 167–170, 1999.
- Logan, J. A., M. J. Prather, S. C. Wofsy, and M. B. McElroy, Tropospheric chemistry: A global perspective, *J. Geophys. Res.*, **86**, 7210–7254, 1981.
- Müller, J. F., Geographical distribution and seasonal variation of surface emissions and deposition velocities of atmospheric trace gases, *J. Geophys. Res.*, **97**, 3787–3804, 1992.
- Müller, J. F., and G. Brasseur, IMAGES: A three-dimensional chemical transport model of the global troposphere, *J. Geophys. Res.*, **100**, 16,445–16,490, 1995.
- Olivier, J. G. J., A. F. Bouwman, C. W. M. Van der Maas, J. J. M. Berdowski, C. Veldt, J. P. J. Bloos, A. J. H. Visschedijk, P. Y. J. Zandveld and J. L. Haverlag, Description of EDGAR Version 2.0: A set of global emission inventories of greenhouse gases and ozone-depleting substances for all anthropogenic and most natural sources on a per country basis and on $1^\circ \times 1^\circ$ grid, National Institute of Public Health and the Environment (RIVM) report no. 771060 002/TNO-MEP report no. R96/119, 1996.
- Smolarkiewicz, P. K., and P. J. Rasch, Monotone advection on the sphere: An eulerian versus a semi-Lagrangian approach, *J. Atmos. Sci.*, **48**, 739–810, 1991.

C. Granier, Service d’Aéronomie, CNRS, Paris, France.
G. P. Brasseur, Max Planck Institute for Meteorology, Hamburg, Germany.